Songklanakarin J. Sci. Technol.
43 (6), 1756-1763, Nov. - Dec. 2021

http://www.sjst.psu.ac.th

Original Article

Analytical method for accelerating time calculation of induction motors using standard technical information♣

Pichai Aree*

Department of Electrical and Computer Engineering, Faculty of Engineering, Thammasat University, Khlong Luang, Pathum Thani, 12120 Thailand

Received: 22 November 2020; Revised: 21 May 2021; Accepted: 25 June 2021

Abstract

Asynchronous or induction motors are commonly employed in industrial applications. Their precise accelerating or starting time is needed for setting their overcurrent protection devices against heating and for assessing power quality of electric utility distribution power system. The accelerating time is usually determined from a tedious time-domain dynamic simulation with commercial software tools, which basically require a full knowledge of the motor's equivalent parameters. Often these parameters are not readily available to the end-users while other technical information is. Thus, this paper presents a novel analytical approach to calculate the motor accelerating time using standard technical data. The required speed-torque curve of induction motors is directly determined from the manufacturer-provided information, instead of requiring the conventional equivalent-circuit parameters. Accuracy of the proposed technique is validated by comparing the calculated accelerating times against those from time-domain dynamic simulations using a full fifth-order model of induction motor: the results mostly agree in a satisfactory manner.

Keywords: accelerating time, accelerating torque, induction motor, speed-torque curve

1. Introduction

Three-phase AC induction motors are primarily employed in commercial and industrial applications because of their simplicity, high reliability, and being almost free of maintenance. Provided a strong grid connection, the cheapest way to start up a high-voltage induction motor is by the direct-on-line method (Vlad, Campeanu, Enache, & Enache, 2017). Due to a high sustained starting current, the motor must accelerate to full speed within the locked-rotor withstand time or safe stall time, irrespective of the type of load (Dsouza *et al.*, 2019; Naik, 2017; Reimert, 2006; Rajendra, Finley, & Gaerke, 2017). Hence, the acceleration or starting times of induction motors are very important, affecting how to set their overcurrent protective devices against overheating (Kay & Padden, 2020; Kolosov, 2020; Rahmani, Niaki, & Sadeghi, 2019). Furthermore, from a power-system planning point of view, it must be ensured that starting a large induction motor would not cause unacceptable voltage sags and flicker, according to the restrictions of the established power acceptability curve, such as that by the Computer & Business Equipment Manufacturers Association (CBEMA) (Wang *et al.*, 2011). Since the voltage-sag duration is closely related to the motor's accelerating time, it can play a significant role to power quality of a power distribution system. Hence, the accelerating time or the related sag duration due to the largest motor starting must be considered in a power quality assessment (Styvaktakis, 2002).

Generally, the accelerating time of an induction motor can be accurately calculated using time-domain dynamic simulation. This approach is quite time-consuming and needs commercial software tools (Oputa, Obi, & Onwuka, 2017; Patil & Porate, 2009). With these tools, the motor's equivalent-circuit parameters are always required for the dynamic simulation. To avoid using the high-cost simulation tools for conducting dynamic simulations, and the problem of identifying the motor's parameters, most of the manufacturers provide a simplified set of formulae to roughly estimate the

♣Peer-reviewed paper selected from The 9th International Conference on Engineering and Technology (ICET-2021)
*Corresponding author
Email address: apichai@engr.tu.ac.th

average value of motor's electrical torque and driven-load torque, so that the accelerating time can be rapidly approximated using first-order dynamics for motion of the induction motor (ABB Motor Guide, 2014; Grundfos, 2004; Rockwell Automation, 2004). However, this simplified approach does not provide an exact value of the accelerating time, since the motor and driven-load torques are simply estimated. From the published technical guidance, this method is rather limited to only three types of mechanical load profiles (lifts, fans, or piston pumps). It cannot be applied with other reduced voltage starting techniques.

To improve the accuracy of accelerating time computation, available torque curves of motor and mechanical load are plotted on a pair of axes in the same figure. Then, a net accelerating torque is calculated by dividing the area between the motor and load torque curves into small equal intervals over the entire range of speeds from standstill to its full running condition (Garg & Tomar, 2015; Rahmani, Niaki, & Sadeghi, 2019). The areas for all intervals are finally added up to get the average accelerating torque, allowing the accelerating time to be estimated. The selected step size or interval length directly determines accuracy of the computational result.

In order to get an accurate accelerating time, reliable speed-torque curves of induction motors are generally required. Conventionally, they can be calculated using a set of the motor's standardized test parameters, mostly taken from field measurements or identifications. To avoid the difficulties with field tests, the motor's parameters can be possibly determined from the manufacturer catalogue information using some nonlinear approach (Perez, Gomez-Gonzalez, & Jurado, 2013; Weiping, Zhang, & Zhou, 2018). However, they may not always converge with all sets of the catalog data (Pedra, 2008). In the same manner, this paper attempts to apply a novel analytical approach to determine the motor's speed-torque curve directly from the available technical information, permitting an accelerating time assessment.

Hence, this paper presents an analytical approach to determine the accelerating time without resorting to time-domain dynamic simulations requiring commercial simulation tools. The analytical formulae are fully developed to compute the speed-torque curve of a motor using technical catalog information, without field-measurement of the equivalent-circuit parameters. This approach gives a rapid determination of the accelerating time. The proposed analytical technique is validated against time-domain dynamic simulations by comparing the accelerating times from both methods.

2. Derivation of motor's speed-torque curve from technical catalog information

In this section, a novel technique to determine the speed-torque curve of a single-cage induction motor is addressed. The available catalog data, consisting of rated torque (T_n), break-down torque (T_b), starting torque (T_{st}), and rated slip (s_n) are regarded as input data. To derive the expression of speed-torque curve, the motor equivalent circuit model in Figure 1 is used. It is convenient to convert the common T-form model into Thevenin's circuit expressed in term of Thevenin's voltage, resistance (R_{th}), and reactance (X_{th}). Then, the motor's electrical torque T_e in Nm can be

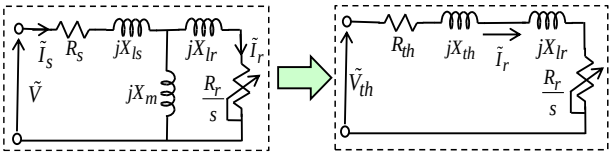

Figure 1. Equivalent circuit model of induction motor

represented as a function of slip (s) with the following three coefficients:

$$T_e = \rho_2 s / (s^2 + \rho_1 s + \rho_0) \quad (1)$$

where,

$$\rho_0 = R_r^2 / (R_{th}^2 + (X_{th} + X_{lr}{}^2)) \quad (2)$$

$$\rho_1 = 2R_{th}\rho_0 / R_r \quad (3)$$

$$\rho_2 = 3V_{th}^2 \rho_0 / (\omega_{sm} R_r) \quad (4)$$

ω_{sm} denotes the mechanical synchronous speed (rad/sec). Thevenin's voltage, resistance, and reactance in Figure 1 can be expressed as,

$$V_{th}^2 = X_m^2 V_n{}^2 / (R_s^2 + (X_m + X_{ls})^2) \quad (5)$$

$$R_{th} = R_s X_m^2 / (R_s^2 + (X_m + X_{ls})^2) \quad (6)$$

$$X_{th} = \frac{R_s X_m^2 + X_{ls} X_m (X_m + X_{ls})}{R_s^2 + (X_m + X_{ls})^2} \quad (7)$$

V_n in (5) indicates rated voltage. R_s and R_r correspond to stator and rotor resistances, respectively. X_{ls}, X_{lr}, and X_m are related to stator leakage, rotor leakage, and mutual reactance, respectively. To determine the speed-torque curve from the motor's catalog information, a pair of operating points related to break-down torque (T_b) at s=s_b and starting torque (T_{st}) at s=1 are needed. Substituting s=1 into (1) gives,

$$T_{st} = \rho_2 / (1 + \rho_1 + \rho_0) \quad (8)$$

Rearranging (8) gives,

$$\rho_2 = T_{st} (1 + \rho_1 + \rho_0) \quad (9)$$

Next, substituting s=s_b into (1) gives,

$$T_b = \rho_2 s_b / (s_b^2 + \rho_1 s_b + \rho_0) \quad (10)$$

By taking the derivative of the torque equation in (10) with respect to slip and setting it to zero, the coefficient ρ_0 can be found in terms of breakdown slip (s_b) as,

$$\rho_0 = s_b^2 \quad (11)$$

Substituting (11) into (10) gives,

$$T_b = \rho_2 / (2s_b + \rho_1) \quad (12)$$

The coefficient ρ_1 can be expressed by equating (8) and (12) as,

$$\rho_1 = (T_{st}(1+s_b^2) - 2s_bT_b)/(T_b - T_{st}) \quad (13)$$

After substituting (11) and (13) into (9), the coefficient ρ_2 can be rearranged to

$$\rho_2 = (T_bT_{st}(1-s_b)^2)/(T_b - T_{st}) \quad (14)$$

It is evident from (11), (13) and (14) that the toque coefficients in (1) can be determined from the technical data on rated, starting, and breakdown torques, as well as rated and breakdown slip. Because the breakdown slip is an unknown variable, it is also estimated from the technical information. According to (1)-(4), the ratio between breakdown and rated torque (T_b/T_n) can be expressed as,

$$\frac{T_b}{T_n} = \frac{s_n^2 + 2s_b^2 s_n R_{th}/R_r + s_b^2}{2s_b s_n (1 + s_b R_{th}/R_r)} \quad (15)$$

Referring to (15), the ratio between Thevenin's and rotor resistances (R_{th}/R_r) is needed. It can be solved from the ratio of breakdown and starting torques (T_b/T_{st}), which can be derived from (1)-(4) as,

$$\frac{T_b}{T_{st}} = \frac{1 + (2R_{th}/R_r)s_b^2 + s_b^2}{2s_b + (2R_{th}/R_r)s_b^2} \quad (16)$$

After rearranging (16), the ratio R_{th}/R_r is given by,

$$\frac{R_{th}}{R_r} = \frac{1 + s_b^2 - 2s_b(T_b/T_{st})}{2s_b^2(T_b/T_{st} - 1)} \quad (17)$$

By substituting (17) into (15), the breakdown slip can be then expressed in terms of a quadratic equation

$$\left(K + \frac{T_n}{s_nT_b}\right)s_b^2 - 2\left(K\frac{T_b}{T_{st}} + 1\right)s_b + \left(K + \frac{T_ns_n}{T_b}\right) = 0 \quad (18)$$

Here,

$$K = (T_n/T_b - 1)/(T_b/T_{st} - 1) \quad (19)$$

Finally, the break-down slip can be found from (18) using the given rated, breakdown, and starting torques, along with rated slip. The breakdown slip is required for determining the accurate speed-torque curve of a single-cage induction motor from its technical data. Since all coefficients in (1) are derived from the motor rated voltage (V_n), they cannot be used for predicting the performance curve under the reduced-voltage starting technique such as with autotransformer or star-delta starter. Hence, the torque equation in (1) can be further modified to

$$T_e = \frac{\rho_2 s}{s^2 + \rho_1 s + \rho_0}(V/V_n)^2 \quad (20)$$

where V is the applied voltage.

3. Validation of Proposed Torque Model

It is interesting to validate the proposed speed-torque model with the given coefficients in (11), (13), and (14) against the exact T-form equivalent circuit in Figure 1. Let us consider the medium voltage induction motor, rated at 4.16kV and 1000HP. A known set of the motor's parameters with conventional equivalent circuit is initially employed to produce the required input technical data, which are starting, breakdown, and rated torques, as indicated in Table 1. The generated data are used instead of the actual technical specifications, because it is easy to check correctness of the proposed model against the exact equivalent-circuit model. Then, the data in Table 1 are applied to calculate the main coefficients ρ_0, ρ_1, and ρ_2 shown in Table 2. The coefficients are further applied to evaluate the speed-torque curves under two different voltages as displayed in Figure 2. The true curves directly generated from the equivalent-circuit parameters are also displayed for comparison. It is noticed from Figure 2 that the speed-torque curves between the equivalent circuit approach and proposed torque model in (20) fully agree for all cases with 100% and 80% applied voltages. The model validation is further carried out using the published technical data of the 4.16kV and 1000HP motor (Ansuj, Shokooh, & Schinzinger, 1989). These technical data are initially employed to evaluate the coefficients ρ_0, ρ_1, ρ_2 shown in Table 3. These coefficients are further applied to compute the speed-torque curve from (20), displayed in Figure 3a. The true curve published in (Ansuj, Shokooh, & Schinzinger, 1989) is also given for comparison. A good agreement between them is found, in a satisfactory manner.

Table 1. Parameters of a 1000HP motor and technical data

Parameters of 1000HP, 60Hz, 4.16kV motor						
R_s, Ω	R_r, Ω	X_{ls}, Ω	X_{lr}, Ω	X_m, Ω	N_r, rpm	J, kg.m^2
0.47	0.63	2.37	3.42	65.22	3510	21
Manufacturer data generated from above set of the parameters						
N_r, rpm		T_n, Nm		T_b, Nm		T_{st}, Nm
3510		1561		3466		798

Table 2. Computed coefficients

ρ_0	ρ_1	ρ_2
1.2102×10^{-2}	1.6812×10^{-2}	8.2104×10^{2}

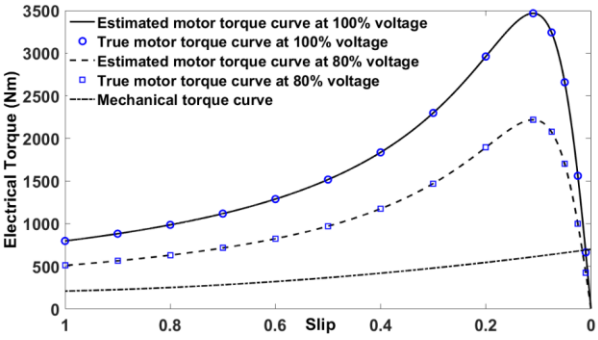

Figure 2. Speed-torque curves for two applied voltages

Table 3. Motor technical data and computed coefficients

HP	Motor manufacturer data						Computed coefficients		
	f	kV	s_n	T_n	T_{st}	T_b	ρ_0	ρ_1	ρ_2
1000	60	4.16	0.015	2008.4	622.6	4317.8	0.00427	0.0164	0.06354
40	50	0.4	0.09	190	260	370	0.13834	0.18844	344.96
5	50	0.4	0.07	25	15	42	0.04003	0.04467	14.93

Moreover, a validation of speed-torque curves is conducted. The computed torque curves are compared against those generated from the equivalent-circuit parameters that are fully obtained from a modified shuffled frog-leaping (MSFL) algorithm (Perez, Gomez-Gonzalez, & Jurado, 2013). The published technical information for 40HP and 5HP single-cage motors as shown in Table 3 is employed. The plots of speed-torque curves from the proposed and the published MSFL method are exhibited in Figures 3b and 3c, respectively. It is found that the torque curves are relatively close to each other. According to the presented results, the model proposed in (20) could be applied to estimate the speed-torque curves of single-cage induction motors with sufficient accuracy, using available catalogue data in the accelerating-time calculation.

4. Analytical Solution of Accelerating Time

The accelerating time of induction motor can be determined from first-order dynamic motion equation (Tooley, 2010),

$$J\frac{2\pi N_s}{60}\frac{dn_r}{dt}=T_{acc} \tag{21}$$

where J is total inertia in kg.m^2, which is sum of motor J_m and driven-load J_L inertias. n_r is per-unit speed, which is the ratio of actual rotor speed N_r to synchronous speed N_s (both in rpm). The acceleration torque T_{acc} is the difference between motor and driven-load torques,

$$T_{acc}=(T_e-T_m) \tag{22}$$

According to the IEEE standard (IEEE Task Force, 1995), the driven-load torque can be expressed as

$$T_m=T_{m0}(A(1-s)^2+B(1-s)+C) \tag{23}$$

where

$$s=(1-n_r) \tag{24}$$

T_{m0} in (23) is torque at synchronous speed. The characteristic of motor driven load can be adjusted to be proportional to speed squared, to speed, or a constant, by choice of the coefficients A, B, and C. By substituting (20) and (23) into (22), the acceleration torque can be expressed in terms of per-unit speed (n_r) as,

$$T_{acc}=\frac{n_r^4+b_3n_r^3+b_2n_r^2+b_1n_r+b_0}{a_2n_r^2+a_1n_r+a_0} \tag{25}$$

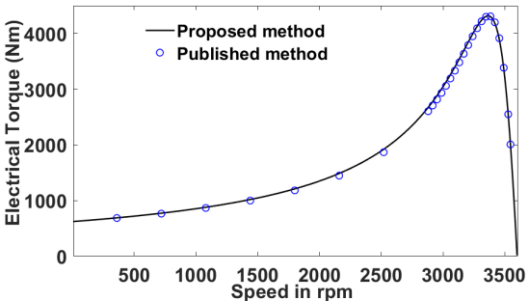

(a) 1000HP motor

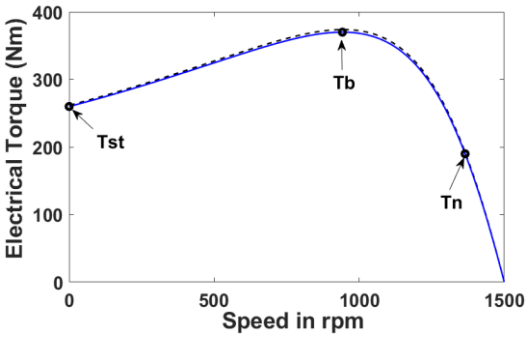

(b) 40HP motor

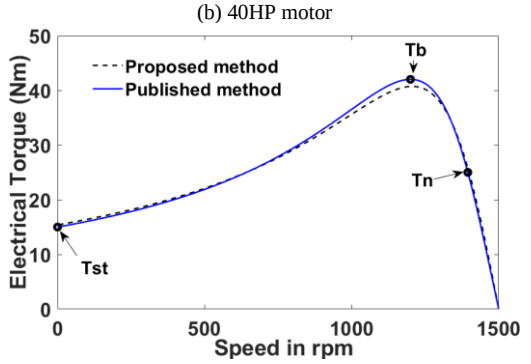

(c) 5HP motor

Figure 3. Comparative speed-torque curves

The coefficients in (25) are listed in Appendix A. After substituting (25) into (21) and re-arranging, the time t_{acc} required for motor to accelerate from rest to any given speed (n_{hi}) can be found as

$$t_{acc}=\frac{2\pi JN_s}{60}\int_0^{n_{hi}}\left(\frac{a_2n_r^2+a_1n_r+a_0}{n_r^4+b_3n_r^3+b_2n_r^2+b_1n_r+b_0}\right)dn_r \tag{26}$$

This can be expressed as a partial fraction

$$t_{acc} = \frac{\pi J N_s}{30} \int_0^{n_{hi}} \left(\frac{k_1}{n_r - n_1} + \frac{k_2}{n_r - n_2} + \frac{k_3}{n_r - n_3} + \frac{k_4}{n_r - n_4} \right) dn_r \quad (27)$$

where

$$k_1 = \frac{a_2 n_1^2 + a_1 n_1 + a_0}{(n_1 - n_2)(n_1 - n_3)(n_1 - n_4)} \quad (28)$$

$$k_2 = \frac{a_2 n_2^2 + a_1 n_2 + a_0}{(n_2 - n_1)(n_2 - n_3)(n_2 - n_4)} \quad (29)$$

$$k_3 = \frac{a_2 n_3^2 + a_1 n_3 + a_0}{(n_3 - n_1)(n_3 - n_2)(n_3 - n_4)} \quad (30)$$

$$k_4 = \frac{a_2 n_4^2 + a_1 n_4 + a_0}{(n_4 - n_1)(n_4 - n_2)(n_4 - n_3)} \quad (31)$$

After integrating (27), the total accelerating time (t_{acc}) of the motor is

$$t_{acc} = \frac{\pi J N_s}{30} \sum_{j=1}^{4} k_j \ln\left(1 - n_{hi} / n_j\right) \quad (32)$$

The accelerating time in (32) can be computed once a set of solutions (n_1, n_2, n_3, and n_4) of the fourth-order polynomial in the denominator of (26) is found. Let n_f denote the per-unit full-load speed (stable equilibrium point) which is in the set $\{n_1, n_2, n_3, n_4\}$. Equation (32) is not valid to compute the accelerating time when the upper speed n_{hi} is exactly equal to the full-load speed n_f since it will go to infinity. To avoid this problem, an upper bound of the integral should not reach the exact value of speed n_f but rather be in the neighborhood of n_f by a factor ε. Thus, the time in which the induction motor accelerates from standstill to full-load speed can be modified to,

$$t_{acc} = \frac{\pi J N_s}{30} \sum_{j=1}^{4} k_j \ln\left(1 - (n_f - \varepsilon) / n_j\right) \quad (33)$$

By trial-and-error it is found that a small value of ε at about 0.0002 is appropriate for computing the accelerating time with sufficient accuracy. The accelerating time calculation of a three-phase single-cage induction motor can be achieved as long as the acceleration torque remains positive for the whole range of running speeds.

5. Step-by-step Procedure of Accelerating Time Calculation

This section gives a step-by-step procedure for calculating the accelerating time. It can be summarized as follows:

1) Preparing the required catalog information of induction motor such as rated, breakdown, and starting torques (T_n, T_b, T_{st}), rated slip (s_n), as well as mechanical load-torque profile described by the coefficients (A, B, C) with the synchronous torque T_{m0} in (23).

2) Computing the break-down slip (s_b) from (18) using the technical information.

3) Computing the coefficients ρ_0, ρ_1, ρ_2 from (11), (13), (14), respectively.

4) Setting equation (25) to zero, then solving for a set of n_r as solutions (n_1, n_2, n_3, n_4) with the aid of (A-1)-(A-7).

5) Computing the accelerating time from (33) after evaluating the coefficients (k_1-k_4) from (28)-(31).

6. Results and Discussion

In this section, the accelerating times calculated from the analytical formula in (33) are compared against those accurately obtained from time-domain dynamic simulation, for validation. First of all, it is interesting to compare for accuracy the accelerating time obtained from a simplified approach (ABB Motor Guide, 2014) against the proposed method, and with time-domain dynamic simulation. Let us choose the simplest profile of the driven-load torque for the 1000HP motor (Table 1) as a constant type with following parameters: T_{m0}=500Nm, A=B=0, C=1.0, for conducting the study. Referring to the manufacturer's guidance material (ABB Motor Guide, 2014), the accelerating time is expressed by t_{acc}=J×K_1/T_{acc}, where the accelerating torque T_{acc} is simply approximated by 0.45×(T_{st}-T_b)-$K_L T_m$. The value of the constant K_1 is 377 for a two pole motor, and the load coefficient K_L is equal to 1.0 for a constant-torque type load. After evaluating the average accelerating torque using breakdown and starting torques from Table 1, the time required to accelerate the 1000HP motor up to full speed is estimated as 5.6 sec. For comparison with the proposed method, the main coefficients ρ_0, ρ_1, ρ_2 in Table 2 are then employed to evaluate the coefficients in (27) as given in (A-1)-(A-7) (Appendix A). These coefficients are applied to solve for all four possible roots (n_1, n_2, n_3, n_4) using the analytical approach in (Zwillinger, 2018). These roots permit calculation of the k-coefficients in (28)-(31) for accelerating time calculation as shown in Table 4 (column 2). It is evident that the analytical formula in (33) gives a solution of the accelerating time of about 10.4 sec. The difference in accelerating time estimates from manufacturer's technical guidance and the proposed method is almost two-fold. Next, to compare with an accurate time-domain dynamic simulation, the fifth-order model of induction motor is employed to generate the speed response shown Figure 4a. It is clearly seen that the motor takes a total time of 10.5 sec to reach a steady-state condition. The computed acceleration times obtained from the proposed method and time-domain simulation agree with each other very well. Thus, the proposed method is far better than the simplified approach found in the manufacturer's technical documentation.

A comparison between the proposed method and dynamic simulation was further conducted with varied applied input voltages. In this study, a more complex mechanical load profile for the 1000HP motor was set via (23) with the following parameters: T_{m0}=700Nm, A=0.5, B=0.2, C=0.3. This profile is plotted in Figure 2. According to Table 4 (columns 3 and 4), the root n_1 is related to the stable equilibrium point. The times required for motor to accelerate

Table 4. Computed coefficients and accelerating times

	T_{m0}=500Nm, A=B=0, C=1	T_{m0}=700Nm, A=0.5, B=0.2, C=0.3	
	100% voltage	100% voltage	80% voltage
n_1	0.9923	0.9895	0.9835
n_2	-0.6216	-0.9813	-0.7397
n_3	-0.6216+j9.9641	0.8042+j1.0644	0.6865+j0.8623
n_4	-0.6216-j9.9641	0.8042-j1.0644	0.6865-j0.8623
k_1	-1.52683×10^{-5}	-1.5381×10^{-5}	-2.5219×10^{-5}
k_2	3.3016×10^{-3}	1.3321×10^{-3}	1.8311×10^{-3}
k_3	-0.0016+j0.00987	$-(6.5837-j2.2343)\times10^{-4}$	$-(9.0295+j1.3794)\times10^{-4}$
k_4	-0.0016-j0.00987	$-(6.5837+j2.2343)\times10^{-4}$	$-(9.0295-j1.3794)\times10^{-3}$
t_{acc}	10.4sec	7.73sec	14.47sec

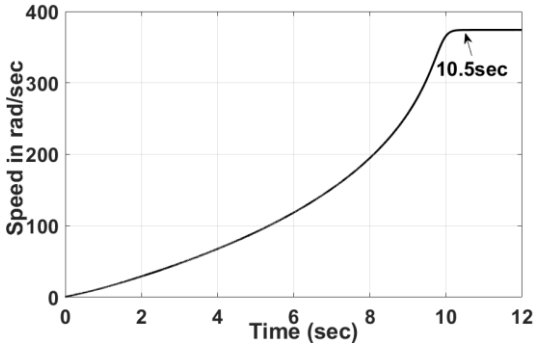

(a) with constant torque load

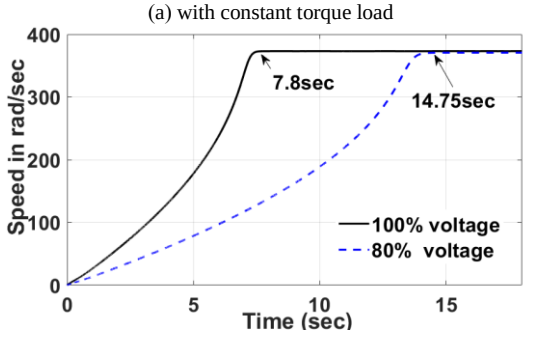

(b) with difference in voltage

Figure 4. Speed responses with 100% and 80% applied voltages

from rest to full speed (n_1) are 7.73 sec and 14.47 sec for the cases with 100% and 80% applied voltages, respectively. To validate the proposed formula in (33), the comparative responses of motor speed taken from the time-domain dynamic simulation are shown in Figure 4b. It is evident that the motor takes 7.8 sec and 14.75 sec to reach the full-load speeds in the cases with 100% and 80% applied voltages, respectively. Thus, the accelerating times obtained from the analytical approach closely agree with those from the time-domain simulations.

Next, validations are further carried out when the mechanical driven-load torque in (23) is increased via the parameter T_{m0} until the motor is almost unable to accelerate. The accelerating time estimates from the analytical and time-domain approaches are plotted against each other in Figure 5. It can be observed that the motor takes longer to accelerate as the mechanical load torque increases. The accelerating time begins to rise rapidly in a quadratic manner with the load torque. At the load-torque level corresponding to the point *a*, the motor acceleration torque is nearly insufficient to bring it up to full speed. For example, referring to Table 1, it is found that the 1000HP motor is capable of supplying the net starting torque of 798Nm. Because the mechanical load requires 95.9% of 798Nm (point *a*), it should come as no surprise that the accelerating time is greatly increased due to a significant reduction in the acceleration torque at locked-rotor condition. At the point a, Figure 5 shows that the computing error (ΔE) between the analytical and time-domain methods is about 6.8%. As the mechanical load torque is increased further up to the critical level at point c (98.9% of 798Nm) until the acceleration torque at the starting condition is almost exhausted, the error (ΔE) is much more pronounced. The growth of error is possibly due to an increase in the degree of motor nonlinearity, causing the simplified first-order model in (21) used for accelerating-time calculation to be inappropriate. It should be noted that the calculation errors are exhibited in the same way for the case of 80% applied voltage. The corresponding errors (ΔE) in Figure 5 are displayed in Figure 6. Most of them lie between 1% and 8% as long as the mechanical load torque does not approach the critical level. Based on the presented results, good agreement of the accelerating time between the proposed method and the time-domain simulations was observed in a satisfactory manner.

6. Conclusions

This paper presented a novel comprehensive analytical approach for estimating the accelerating time, required for setting the overcurrent protective devices of a single-cage induction motor. This approach allows the motor's speed-torque curve to be computed straightforwardly from commonly offered catalogue information, without the need for conventional equivalent-circuit parameters. With the presented analytical formulae, the calculation of a motor's accelerating time is easily done without the conventional commercial simulation tools. According to the presented results, good agreement of the accelerating time estimates between the proposed analytical method and time-domain dynamic simulations was observed, in a satisfactory manner. Hence, the proposed method is useful for the rapid estimation of accelerating time, assisting engineers to set the protective overcurrent devices of induction motors, and to assess the power quality of power distribution system when affected by starting the motor. It should be noted that the proposed technique is capable of evaluating the accelerating time under

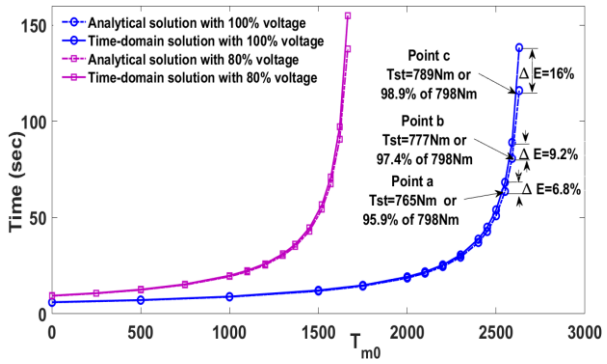

Figure 5. Accelerating times from analytical and time-domain approaches

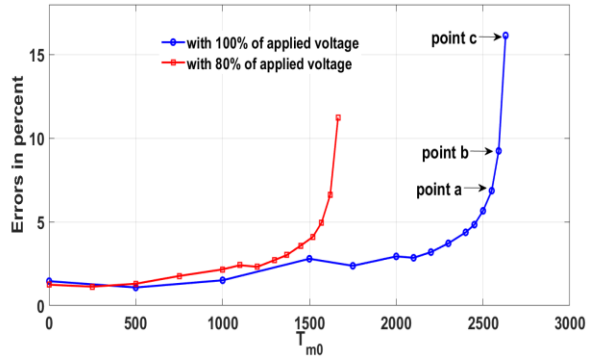

Figure 6. Errors in the computed accelerating times

voltage sag produced by the motor starting, once the voltage magnitude at the point of common coupling is determined using the motor's locked-rotor current before plugging it into the proposed torque formula. Moreover, for hot starts when a motor is restarted after reaching its normal operating temperature, the acceleration time may not be correctly estimated because the developed torque formula does not take into account temperature rise effects on rotor resistance. Also, this approach is not well suited for modern AC drives since the motor's accelerating time is directly determined by the ramp-up control implemented in most V/F inverters. Finally, the developed analytical formula could be further employed to generate the speed-torque curve, offering a proper selection of single-cage motors to match their mechanical drive loads.

Acknowledgements

The author gratefully acknowledges the financial support provided by Faculty of Engineering, Thammasat University, contract No. 001/2563.

References

ABB Motor Guide. (2014). *Basic technical information about low voltage standard motors.* Zurich, Switzerland: ABB Motor

Ansuj, S., Shokooh, F., & Schinzinger, R. (1989). Parameter estimation of induction machines based on sensitivity analysis. *IEEE Trans. Industrial Applications*, *25*(6), 1035-1040.

Dsouza, M., Al-Turki, M., & Safwa, M. (2019). Power system design for a large, dynamic natural gas filed: improving the field production profile. *IEEE Industry Applications Magazine*, *25*(5), 35-46.

Grundfos. (2004). *Motor book*. Bjerringbro, Denmark: Grundfos Management A/S.

Garg, A., & Tomar, A. S. (2015) Starting time calculation for induction motor. *International Journal of Engineering Research and Application*, *5*(5), 56-60.

IEEE Task Force. (1995). Load representation for dynamic performance. *IEEE Trans. Power Systems*, *10*(3), 1302-1313.

Kay, J. A., & Padden, L. K. (2020). Review of the new IEEE STD. 3004.8 "Recommended practice for motor protection in industrial and commercial power system" with focus on forest products industries. *IEEE Trans. Industrial Applications*, *56*(4), 3350-3358.

Kolosov, G. (2020). *Protection settings and selectivity in industrial networks* (Diploma Thesis, Technical University of Ostrava, Ostrava, Czech) Retrieved from https://dspace.vsb.cz/bitstream/handle/10084/140483/KOL0452_FEI_N2649_3907T001_2020.PDF?sequence=1

Mitsubishi, *FATEC Inverter Practical Course*. Tokyo, Japan: Mitsubishi Electric Corporation.

Naik, S. (2017, October 2). Understanding the importance of torque-speed curve and load inertia for motor selection, *Synergy Robotics and Motion Newsletter*, 1-4.

Oputa, O., Obi, P. I., & Onwuka, I. K. (2017). Induction motor starting analysis and start aided device comparison using ETAP. *European Journal of Engineering Research and Science*, *2*(7), 1-7.

Patil, P. S., & Porate, K. B. (2009). Starting analysis of induction motor: A Computer simulation by ETAP power station. *Proceeding of the* 2nd *International Conference Emerging Trends in Engineering and Technology (ICETET)*, 494-499.

Pedra J. (2008) On the determination of induction motor parameters from manufacturer data for electromagnetic transient programs. *IEEE Trans. Power Systems*, *23*(4), 1709-1718.

Perez, I., Gomez-Gonzalez, M., & Jurado, F. (2013). Estimation of induction motor parameters using shuffled frog-leaping algorithm. *Electrical Engineering*, *95*, 267–275.

Rahmani, R., Niaki, A. A., & Sadeghi, S. H. H. (2019). Large induction motor starting time determination for the purpose of protection coordination. *Proceeding of the* 27th *Iranian Conference on Electrical Engineering*, 475-480.

Rajendra, M., Finley, W. R., & Gaerke, G. (2017). Comparison of IEC and NEMA requirements to ensure proper specification and design of induction motors & generators for global use. *Petroleum and Chemical Industry Technical Conference*, 35-44.

Reimert, D. (2006). *Protective relay for power generation system*. Florida, Fl: Taylor and Francis.

Rockwell Automation. (2004). *Application basic of operation of three-phase induction motors: Design duty types selection dimensioning*. Schenectady, NY: Power

Technologies Inc.
Styvaktakis, E. (2002). *Automating power quality analysis, Chalmers University of Technology* (Technical Report No. 423).
Tooley, M. (2010). *Plant and Process Engineering*. Oxford, England: Butterworh-Heinemann.
Vlad, I., Campeanu, A., Enache, S., & Enache, M. A. (2007). Study of direct-on-line starting of low power asynchronous motors, *International Conference on Electromechanical and Power Systems (SIELMEN)*, Chisinau, Republica Moldova, 137-142
Wang, X., Yong, J., Xu, W., & Freitas, W. (2011). Practical power quality charts for motor starting assessment. *IEEE Transactions on Power Delivery*, 26(2), 799-808.
Weiping, L., Zhang, Y., & Zhou, R. (2018). Parameters identification of induction motor model based on manufacturer data and sequential quadratic programming. *Automation, Control and Intelligent Systems*, *6*(3), 28-37.
Zwillinger, D. (2018). *Standard Mathematical Tables and Formulae* (32nd ed.). Florida, FL: CRC press.

Appendix

This appendix provides a list of coefficients in (26)

$$a_2 = -1/(AT_m^0) \quad \text{(A-1)}$$

$$a_1 = (2+\rho_1)/(AT_m^0) \quad \text{(A-2)}$$

$$a_0 = -(1+\rho_0+\rho_1)/(AT_m^0) \quad \text{(A-3)}$$

$$b_3 = a_1/a_2 + B/A \quad \text{(A-4)}$$

$$b_2 = a_0/a_2 + a_1 B/a_2 A + C/A \quad \text{(A-5)}$$

$$b_1 = a_0 B/a_2 A + a_1 C/a_2 A + \rho_2 (V/V_n)^2/(AT_m^0) \quad \text{(A-6)}$$

$$b_0 = a_0 C/a_2 A - \rho_2 (V/V_n)^2/(AT_m^0) \quad \text{(A-7)}$$

Nomenclature

T_n, T_b, T_{st}	rated, break-down, starting torque (Nm)
T_e, T_m, T_{acc}	electrical, mechanical, accelerating torque (Nm)
s_n, s_b	rated, break-down slip
V_n, V_{th},	rated, Thevenin's voltage (volt)
R_{th}, X_{th}	Thevenin's resistance, reactance (ohm)
R_s, R_r	stator, rotor resistance (ohm)
X_{ls}, X_{lr}, X_m	stator leakage, rotor leakage, mutual reactance (ohm)
J	inertia (kg.m^2)
N_s, N_r	synchronous, rotor speed (r.p.m.)
n_r	rotor speed (per unit)
A, B, C	torque coefficients
T_{m0}	mechanical torque at synchronous speed (Nm)